J. Am. Chem. Soc. **1994**, *116*, 2281-2291

Examination of the Exchange Interaction through Micelle Size. 2. Isotope Separation Efficiency as an Experimental Probe

Valery F. Tarasov,[*,†] **Naresh D. Ghatlia,**[‡,⊥] **Nickolai I. Avdievich,**[§] **Iliya A. Shkrob,**[∥] **Anatolii L. Buchachenko,**[†] **and Nicholas J. Turro**[*,‡]

Contribution from the Department of Chemistry, Columbia University, New York, New York 10027, Institute of Chemical Physics, Russian Academy of Sciences, Moscow 117334, Russia, International Tomography Center, Novosibirsk 630090, Russia, and Chemistry Division, Argonne National Laboratory, Argonne, Illinois 60439

Received August 5, 1993. Revised Manuscript Received December 30, 1993[•]

Abstract: The geminate reaction probabilities (for recombination and disproportionation) of benzoyl/*sec*-phenethyl radical pairs, generated by the photolysis of α-methyldeoxybenzoin, for both unlabeled (^{13}C in natural abundance at the carbonyl position) and labeled ketones (^{13}C in the carbonyl position) were measured in different sized alkyl sulfate micelles (sodium octyl sulfate (C_8) through sodium dodecyl sulfate (C_{12})) in zero and high magnetic fields (B = 2400 G). Although the probability of geminate recombination (P_r) diminishes for the unlabeled pair, from 0.549 to 0.436 and for the labeled pair from 0.585 to 0.504 at zero magnetic field with decreasing micelle size (C_{12} to C_8), the efficiency of isotope separation (α) is found to increase at zero magnetic field from 1.144 to 1.236 with decreasing micelle size. Theoretical considerations of these experimental results show that the rate of geminate reaction of the unlabeled radical pairs in small micelles is sensitive to the electron spin exchange interaction; intersystem crossing is influenced by fast forced reencounters. These effects are not as important for the labeled radical pairs (which possess a strong ^{13}C hyperfine interaction). In addition, paramagnetic relaxation due to anisotropic hyperfine and electron–electron dipole interactions is shown to be important in the quantitative description of the micelle size dependence of the reaction ability of the labeled radical pairs.

Introduction

In the first paper in this series,[1] we reported an investigation of the influence of micelle size on the geminate recombination probability (P_r) of two different radical pairs (RPs) which may be considered as prototypes of triplet geminate pairs derived from the photolysis of alkyl aryl ketones.[2] We generated radical pairs in aqueous micellar solutions of sodium alkyl sulfates of different hydrocarbon chain lengths [CH_3–$(CH_2)_{n-1}$–$OSO_3^-Na^+$, (C_n, with n = 8–12)]. The photolysis of α-methyldeoxybenzoin (MDB) was employed to produce the benzoyl/*sec*-phenethyl [$C_6H_5CO^\bullet$/$^\bullet CH(CH_3)C_6H_5$] geminate pair. This pair is known[1,2a] (Scheme 1) to undergo three geminate reactions: (1) recombination to reform the bond that fragmented upon α-cleavage; (2) disproportionation to form benzaldehyde and styrene; and (3) combination to form a "head-to-tail" isomer of MDB which is unstable and rearranges to produce 4-ethylbenzophenone; the probabilities for each of these processes are P_r, P_d, and P_{ht}, respectively, and their values can be related conveniently to a theoretical model.[1] These processes compete with radical escape into the bulk aqueous phase, *meso*- and *d,l*-2,3-diphenylbutanes (DPB) are the major products produced by the reaction of random RPs of two *sec*-phenethyl radicals.

We found[1] that the P_r values for the radical pair derived from MDB decrease monotonically as the micelle size decreases from C_{12} to C_8. A comparison between the experimentally determined values of P_r and those calculated within the framework of the microreactor model of the micelle[3,4] revealed that the decrease in P_r with decreasing micelle size can be attributable to the electron spin exchange (ESE) interaction between the uncoupled electrons of the geminate partners. However, the escape rate of radicals from micelles increases as the micelle size gets smaller. Also, the micellar viscosity varies as a function of micellar size. The influences of both of these factors on P_r have been explicitly considered.[1]

The photolysis of 2,4-diphenylpentan-3-one was employed in the previous paper[1] to generate the phenethylacyl/*sec*-phenethyl [$C_6H_5CH(CH_3)CO^\bullet$/$^\bullet CH(CH_3)C_6H_5$] geminate pair. This pair possesses a significantly shorter lifetime than the benzoyl/*sec*-phenethyl pair due to the rapid rate of decarbonylation of the phenethylacyl partner. We chose this system in order to restrict the arbitrariness in the choice of the theoretical adjustable parameters and to subject the theoretical model of micellized RPs to as severe a test as possible. However, the theoretical calculations still required a number of assumptions concerning some parameters that are not directly accessible experimentally. Therefore, further experimental and theoretical efforts are necessary in this context to formulate the most important characteristics and peculiarities of spin selective chemical reactions in microreactors or supercages. These peculiarities are the subject of supramolecular photochemistry.[5]

In this report, we investigate the influence of the micelle size on the geminate reaction probability ($P = P_r + P_d$) of two

---

[‡] Columbia University.

[†] Russian Academy of Sciences.

[§] International Tomography Center.

[∥] Argonne National Laboratory.

[⊥] Present address: Unilever Research, USA, Edgewater, NJ 07020.

[•] Abstract published in *Advance ACS Abstracts*, February 15, 1994.

(1) Tarasov, V. F.; Ghatlia, N. D.; Buchachenko, A. L.; Turro, N. J. *J. Am. Chem. Soc.* **1992**, *114*, 9517.

(2) (a) Heine, H. G.; Hartman, W.; Kory, D. R.; Magyar, J. G.; Hoyle, C. E.; McVey, J. K.; Lewis, F. D. *J. Org. Chem.* **1974**, *39*, 691. (b) Turro, N. J. *Modern Molecular Photochemistry*; University Science Park: Mill Valley, CA, 1991. (c) Turro, N. J. *Tetrahedron* **1982**, *38*, 809. (d) Turro, N. J.; Mattay, J. *J. Am. Chem. Soc.* **1981**, *103*, 4204.

(3) (a) Gosele, V.; Klein, U. K. A.; Hauser, M. *Chem. Phys. Lett.* **1980**, *68*, 291. (b) Hatlee, M. D.; Kozak, J. J.; Rothenberger, G.; Infelta, P. D.; Gratzel, M. *J. Phys. Chem.* **1980**, *84*, 1508. (c) Tachiya, M. In *Kinetics of Nonhomogeneous Processes. A Practical Introduction for Chemists, Biologists, Physicists and Material Scientists*; Freeman, G. R., Ed.; John Wiley: New York, 1987; pp 575–650.

(4) (a) Luders, K.; Salikhov, K. M. *Chem. Phys.* **1985**, *98*, 259. (b) Tarasov, V. F.; Buchachenko, A. L.; Maltsev, V. I. *Russ. J. Phys. Chem.* **1981**, *55*, 936. (c) Sterna, L.; Ronis, D.; Wolfe, S.; Pines, A. *J. Phys. Chem.* **1980**, *73*, 5493. (d) Shkrob, I. A.; Tarasov, V. F.; Buchanchenko, A. L. *Chem. Phys.* **1991**, *153*, 443.

(5) *Frontiers in Supramolecular Organic Chemistry and Photochemistry*; Schneider, H.-J., Dürr, H., Eds.; VCH Publishers: Weinheim, Germany, 1991.

0002-7863/94/1516-2281$04.50/0

Scheme 1. Reaction Pathways for the Geminate Radical Pair Derived from MDB

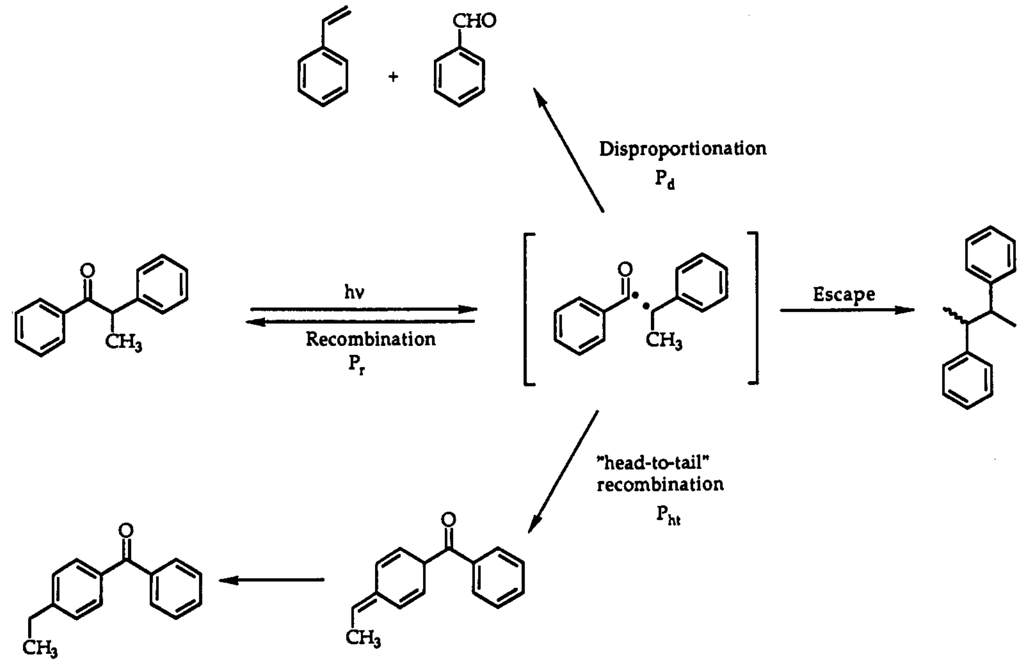

isotopomeric benzoyl/*sec*-phenethyl RPs that are chemically identical and differ only in the magnitude of the hyperfine interaction (HFI) due to an isotopic ^{13}C label at the carbonyl group of the benzoyl radical: $C_6H_5{}^{12}CO^\bullet/{}^\bullet CHCH_3C_6H_5$ and $C_6H_5{}^{13}CO^\bullet/{}^\bullet CHCH_3C_6H_5$. We denote the unlabeled geminate radical pair as RP and the labeled pair as RP*. The probability of geminate reaction of the unlabeled pair is *P* and that of the labeled pair is *P**.

The ^{13}C carbonyl carbon in the benzoyl radical possesses a strong HFI (A = 124 G),[6a] which far exceeds the HFIs due to the H_β (A = 17.9 G)[6a] and H_α (A = −16.3 G)[6a] protons of the *sec*-phenethyl fragment, which in turn far exceed the HFI interactions due to the aromatic protons ($|A| < 6$ G). This special feature of the RP* allows for a simplification of our computation model, especially as applied to a weak magnetic field. As in the high field approximation, the relative contribution (vs that of the ^{13}C) to level mixing due to the HFI of the protons is small. We anticipate that the sacrifice in accuracy due to this approximation will be compensated for by the possibility of considering the role of paramagnetic relaxation in the geminate pair due to both anisotropic HFI (HFI_{aniso}) and electron–electron dipole–dipole interactions (DDI). These relaxation processes were not considered in the previous study.

Besides being part of a continuing effort to develop an appropriate microreactor (supercage) model for micelles, this comparative investigation of chemically identical but isotopically magnetically labeled geminate pairs is also an attempt to understand the most important factors responsible for the efficiency of isotope separation due to the magnetic isotope effect (MIE).[7] Although a high efficiency of ^{13}C isotope separation in micellar geminate recombination reactions[8] was discovered as early as 1978, the details of the MIE mechanism leading to a high efficiency of isotope separation are still not clear. In fact, all reported attempts to explain this phenomenon[4b,c,7b] have actually ignored and/or failed[9] to explain a puzzling experimental observation, i.e., the geminate radical pair in small micelles decays much more slowly than expected on the basis of the models. We propose in this paper that the rate of spin selective reactions in micellized pairs may be *decelerated* if the encounter frequency properly couples with the ESE. If this indeed proves to be the case, then the theoretical interpretation of isotope separation[4b,d,7] in micelle solutions due to MIE needs to be substantially modified.

The rate of encounters of the radicals and the ESE modulated rate of intersystem crossing (ISC) due to the HFI are comparable in magnitude in smaller micelles. Therefore, it is worth speculating whether the rate of encounters can be made to become the rate limiting feature of the geminate pair reaction by increasing the rate of ISC due to a stronger HFI provided by the ^{13}C nucleus in RP*. This feature of either ISC or reencounters being reaction rate determining is quite analogous to the situation for large flexible biradicals for which the rate limiting step for "geminate pair" reaction can be either spin or chain dynamics.[10]

The major experimental observables that we have monitored are (1) the efficiency of photoracemization of optically active MDB and MDB*; (2) the yield of the disproportionation product, benzaldehyde; (3) the yield of the product of escape of the *sec*-phenethyl radicals—diphenyl butanes (DPB); and (4) the efficiency of $^{13}C/^{12}C$ isotope separation. We measure each of these observables as a function of the detergent chain length in zero and in a high external magnetic field (B_0 = 2400 G).

Experimental Section

Gas chromatographic (GC) analyses were carried out using a Hewlett Packard 5890 gas chromatograph equipped with a flame ionization detector, a 25-m SE-30 capillary column, and a Hewlett Packard 3392 electronic integrator. Gas chromatographic–mass spectral (GC–MS) analyses were performed on a Hewlett Packard 5890 gas chromatograph, equipped with a 25-m SE-30 capillary column and a Hewlett Packard 5988 mass selective detector interfaced to a Hewlett Packard 9136 workstation. Mass spectra were acquired in the electron impact ionization mode.

Optically active MDB and MDB* were prepared from optically active L-alanine (Aldrich Chemical Co.) and ^{13}C-labeled L-alanine (99% label, Cambridge Isotopes Ltd.) as reported by Mckenzie et al.[11] d_4-Labeled L-alanine was prepared by a bacterial synthesis in D_2O. This labeled alanine was converted to the d_4-MDB as described for the synthesis of

---

[6] (a) *Landolt-Bornstein*: *Organic C Centered Radicals*; Fisher, H., Hellwege, K.-H., Eds.; Springer-Verlag: Berlin, 1977; Vol. 1, Part b. (b) Holmberg, R. M. *J. Chem. Phys.* **1969**, *65*, 423.

[7] (a) Turro, N. J.; Krauetler, B. *Acc. Chem. Res.* **1980**, *13*, 369–377. (b) Buchachenko, A. L. *Prog. React. Kinet.* **1984**, *13*, 163.

[8] Turro, N. J.; Kraeutler, B. *J. Am. Chem. Soc.* **1978**, *100*, 7432.

[9] (a) Tarasov, V. F.; Shkrob, I. A. *Khim. Phys.* **1990**, *9*, 812. (b) Shkrob, I. A.; Tarasov, V. F. *Chem. Phys.* **1990**, *147*, 369.

[10] (a) Closs, G. L.; Redwine, O. D. *J. Am. Chem. Soc.* **1985**, *107*, 6131. (b) Closs, G. L.; Miller, R.; Redwine, O. D. *Acc. Chem. Res.* **1985**, *18*, 196.

[11] McKenzie, A.; Roger, R.; Wills, G. O. *J. Chem. Soc.* **1927**, 779.

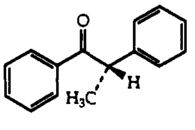

MDB

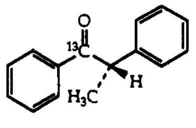

MDB*

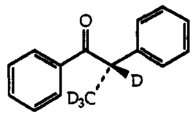

d$_4$-MDB

optically active MDB. The 46.4% isotopically enriched (^{13}C in the carbonyl position) material, obtained by diluting the labeled material with the unlabeled material, was used for the isotope separation experiments.

Sodium dodecyl sulfate (C$_{12}$) was obtained from Bio-Rad and used as received. All other detergents, sodium *n*-undecyl sulfate (C$_{11}$), sodium *n*-decyl sulfate (C$_{10}$), sodium *n*-nonyl sulfate (C$_9$), and sodium *n*-octyl sulfate (C$_8$), were obtained from Lancaster Synthesis and were purified by recrystallization from ethanol–ether mixtures. The concentration of methyldeoxybenzoin used was ~3.3 mM; the concentrations of the detergents used maintained the concentration of micelles at 1.6 mM and the occupancy number of ketone molecules per micelle approximately constant.

Photolyses, with filtered light ($\lambda > 310$ nm) from a 1000-W high-pressure Xe–Hg lamp, were performed on aqueous micellar solutions of MDB which were thoroughly purged with argon prior to and during photolysis. The photolysates were extracted with a mixture of methylene chloride and ethyl acetate, a known amount of a GC standard (dibenzyl ketone or 4-methylbenzophenone) was added, and the samples were dried over MgSO$_4$ and then analyzed by capillary GC–MS to measure the extent of conversion and the isotope content of the substrate ketone. The ions with $m/e = 210$ and 211 were detected in the single ion monitoring mode.

The optical purities of MDB and MDB* were measured either by circular dichroism (CD) analysis of the crude photolysates or by chromatographic analysis using a chiral HPLC column. The CD spectra, of the photolyzed solutions which had been diluted three times with a stock SDS solution, were acquired on a Jasco J-500A spectrometer. The presence of the detergent was shown not to perturb the linear response of the CD spectra of MDB to the enantiomeric excess. The chiral HPLC analyses were performed on a Chiralcel OD-H analytical column (25 cm, 4.5-mm i.d.) using 0.15% isopropyl alcohol in hexane as the eluent. The insert of Figure 1 shows that this column allows for an excellent enantiomeric resolution. The treatment[13a] of the experimental variation in the concentration of enantiomers (Figure 1) during the photolysis does not reveal any preference for the recombination to generate the parent optical isomer. These results using both HPLC and CD methods were identical within the experimental error.

The magnetic field ($B_0 = 2400$ G) photolyses were carried out between the poles of an Alpha Scientific electromagnet. The field strength was measured with a Bell 620 gaussmeter.

Connection between Experimental Observations and Theoretical Parameters. Because of the occurrence of the MIE, isotopomers which possess different magnetic isotopic compositions (molecules with different numbers and/or kinds of isotopic magnetic nuclei in different positions of the RP) will undergo different extents of conversion for identical absorbed doses of light. The conversions of the different isotopomers may be related[13] by eq 1, where f denotes the conversion of the ketone

$$\log(1-f) = \alpha_i \log(1-f_i) \qquad (1)$$

which does not have a ^{13}C nucleus in its skeleton ($m/e = 210$), f_i denotes the conversion of the ketone of the i^{th} specific isotopic composition (m/e 211, 212, ..., 225), and α_i is the efficiency of the isotope separation.

The magnitude of α_i can be related to the probabilities P_{ir} of recombination in the RP with the i^{th} isotopic composition; P_r denotes the recombination probability of the RP which does not contain a ^{13}C nucleus in its skeleton.[13b]

$$\alpha_i = (1-P_{ir})/(1-P_r) \qquad (2)$$

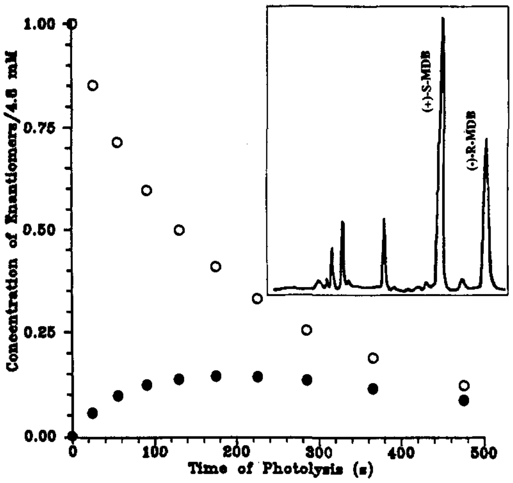

Figure 1. Variation in the concentration of the two optical isomers of MDB during photolysis in C$_{12}$ micelles in zero magnetic field: ○, (+)-(*S*)-MDB; ●, (–)-(*R*)-MDB. Insert shows the resolution of the two optical antipodes using chiral HPLC.

Since conversions in the enrichment experiments have been measured using only the GC–MS data ($m/e = 210$ and 211), we selectively and distinctively measured the conversions of unlabeled and mono-^{13}C labeled material only.

All 15 possible isotopic compositions with one ^{13}C nucleus contribute to the integral intensity of the peak with $m/e = 211$. The ^{13}C content in all positions except for the labeled carbonyl group is equal to the natural abundance value of 0.011. The initial content of ^{13}C in the carbonyl group is 0.866, and hence to calculate f^*, in the conversion of MDB*, which possesses a ^{13}C only in the carbonyl group, we can neglect the change (but not the content itself) in the isotope content at any position other than the carbonyl group despite the fact that such changes actually occur (as has been demonstrated experimentally in the photolysis of dibenzyl ketone[14]).

An important benefit of using an optically active ketone is that it allows for an absolute experimental determination of P_r or P_r^*. Since MDB has a chiral center at the site of bond cleavage, recombination of RP to form MDB leads to photoracemization[15a] of the ketone (Scheme 1). The efficiency of photoracemization may be expressed[13a,15b] by

$$\log(q/q_0) = S\log(1-f_s) \qquad (3)$$

where

$$S = P_r/(1-P_r) \qquad (4)$$

In eq 3, q is the enantiomeric excess of the ketone after photolysis (q_0 is the initial enantiomeric excess) and f_s is the total (substrate + enantiomer) ketone conversion.

The chemical yield (χ_i) of any product of geminate reaction can be expressed in terms of P_r, and the probability of the i^{th} reaction (P_i) as given by eq 5. Using eq 5 it is possible to measure P_d, by monitoring the

$$\chi_i = P_i/(1-P_r) \qquad (5)$$

chemical yield of benzaldehyde (χ_d) as a function of micelle size, HFI, and applied external field.

Equations 1 and 3 are not a simple consequence arising from an assumed monoexponential decay of the RP; these equations may be applied to any form of kinetics. However, the validity of interpreting the experimental data using eqs 2, 4, and 5 is strongly dependent on the assumption that photoracemization of MDB occurs only through geminate pair radical reactions and that all other measured recombination processes of the RP (Scheme 1) also occur in a geminate manner. For example, if photoracemization occurred through nonradical processes, such as photoenolization, errors would result in the application of eq 4. This assumption was verified as shown below.

---

(12) (a) Steiner, U. E.; Wolff, H.-J. In *Photochemistry and Photophysics*; Rabek, J. F., Scott, G. W., Eds.; CRC Press: Boca Raton, FL, 1991; Vol. IV. (b) Steiner, U. E.; Ulrich, T. *Chem. Rev.* **1989**, *89*, 51. (c) Salikhov, K. M.; Molin, Y. N.; Sagdeev, R. Z.; Buchachenko, A. L. *Spin Polarization and Magnetic Effects in Radical Reactions*; Elsevier: Amsterdam, 1984.

(13) (a) Tarasov, V. F.; Ghatlia, N. D.; Buchachenko, A. L.; Turro, N. J. *J. Phys. Chem.* **1991**, *95*, 10220. (b) Tarasov, V. F. *Russ. J. Phys. Chem.* **1980**, *54*, 2438. (c) Bernstein, R. B. *J. Phys. Chem.* **1952**, *56*, 893.

(14) (a) Turro, N. J.; Chung, C.-J.; Lawler, R. G.; Smith, W. J., III. *Tetrahedron Lett.* **1982**, *23*, 3223. (b) Tarasov, V. F.; Buchachenko, A. L. *Bull. Acad. Sci. USSR, Div. Chem. Sci.* (*Engl. Transl.*) **1983**, *32*, 92.

(15) (a) Lewis, F. D.; Magyar, J. G. *J. Am. Chem. Soc.* **1973**, *95*, 5973. (b) Tarasov, V. F.; Shkrob, I. L.; Step, E. N.; Buchachenko, A. L. *Chem. Phys.* **1989**, *135*, 404.

Table 1. Experimental Values of Observables[a]

n[b]	S*[c]	S[c]	χ_d*[d]	χ_d[d]	χ_e*[e]	χ_e[e]
12	1.407	1.216	0.252	0.240	0.060	0.069
	(0.784)	(0.711)	(0.183)	(0.171)	(0.117)	(0.141)
11	1.391	1.443	0.258	0.227	0.060	0.076
	(0.814)	(0.727)	(0.194)	(0.180)	(0.132)	(0.149)
10	1.309	1.058	0.290	0.240	0.066	0.085
	(0.780)	(0.662)	(0.190)	(0.171)	(0.136)	(0.167)
9	1.137	0.907	0.252	0.220	0.076	0.118
	(0.745)	(0.545)	(0.204)	(0.166)	(0.136)	(0.165)
8	1.015	0.774	0.239	0.193	0.083	0.132
	(0.688)	(0.482)	(0.189)	(0.142)	(0.148)	(0.200)

[a] The values in parentheses are those measured at 2400 G. [b] The number of carbon atoms in the detergent chain. [c] Ten different conversions were used in each determination of S and S*. The maximum error in these values is 2%. [d] Values determined for conversions less than 30% (3–4 measurements). The maximum error in these values is 6%. [e] χ_e is independent of conversions. Maximum error in these values is 4%.

Table 2. Comparison of Directly Measured Efficiency of Isotope Separation α with That Calculated (α_{mic}) from Corresponding Probabilities of Recombination[a]

n[b]	P_r*	P_r	α[c]	α_{mie}[d]
12	0.585	0.549	1.144	1.086
11	0.582	0.534	1.128	1.116
10	0.567	0.514	1.142	1.122
9	0.532	0.476	1.171	1.121
8	0.504	0.436	1.236	1.136

[a] Measurements were done in zero magnetic field. [b] Number of carbon atoms in the hydrocarbon chain. [c] Seven different conversion were used in these determinations. Maximum error is ±0.012. [d] Calculated according to eq 2.

Demonstration of the Exclusive Geminate Nature of the Observed Products. Comparison of the experimental results with theory and the use of eq 4 require that the reactions being investigated (Scheme 1) occur exclusively from the geminate pairs produced by α-cleavage. In order to establish the fact that recombination of the RP to generate MDB and disproportionation to generate benzaldehyde do not take place in random RP reactions, MDB was photolyzed in SDS (C_{12}) micelles in a zero external field in the presence of $CuCl_2$, an efficient hydrophilic scavenger (present only in the Stern layer and in the bulk aqueous phase) of *sec*-phenethyl radicals that escape from the micelle. Since P_r characterizes the fate of the RP and not that of the substrate ketone, the influence of $CuCl_2$ on the quantum yield of photodissociation is not relevant to this study. At concentrations of $CuCl_2$ (10 mM), large enough to completely suppress the formation of DPB, formed by the coupling of two *sec*-phenethyl radicals, the values of P_r as well as those of χ_d were identical, within the experimental error, to those measured in the absence of $CuCl_2$. Similar results were obtained when MDB was photolyzed in hexadecyltrimethylammonium chloride micelles. To provide support for the result that benzaldehyde is generated only through RP disproportionation, we photolyzed MDB-d_4 in C_{12} micelles and MDB in D_2O solutions of perdeuterated C_{12}. Extrapolation to zero conversion, after accounting for the photosensitized H/D exchange[16] of the aldehydic proton, shows that at least 80% of the benzaldehyde results from disproportionation.

The application of eq 4 would also be limited if MDB underwent photoreduction by hydrogen abstraction from the detergent chain to form a ketyl radical, since this radical may[17] disproportionate to form an enol which, in turn, could subsequently ketonize to regenerate racemized MDB. However, GC–MS measurements on MDB recovered from partial photolysis in D_2O solutions of perdeuterated SDS show no detectable level of deuterium incorporation in the recovered MDB. Thus, we neglect the possibility of reversible photoreduction of the ketone by the micelle as a significant pathway for racemization of MDB. Finally, photolysis of MDB in homogeneous solution (methanol) did not lead to any significant photoracemization of MDB. Therefore, all conclusions above are applicable to other micelles.

The results from the above experiments strongly support the assumption that the recombination of the RP and their disproportionation take place through the intermediacy of geminate radical pairs so that the values of P_r (P_r*) obtained from S (S*) using eq 4 are experimentally justified. The measured S (S*) and χ_d (χ_d*) values from both the zero and high field experiments in different alkyl sulfate micelles are presented in Table 1. The values of P_r*, P_r, α, and α_{mie}, measured in zero magnetic field, are presented in Table 2.

Correlation between Experimental Parameters. Table 2 shows that the efficiencies of isotope separation estimated indirectly (α_{mie}) using the values of P_r and P_r* and eq 2 are systematically smaller than those measured directly (α) using mass spectroscopy (eq 1). The reason for this discrepancy lies in the fact that eq 2 is derived from consideration of processes related to the recombination step only, whereas α measures the net contribution of all mechanisms that can lead to isotope separation, including effects which occur in the processes of photoexcitation and photodissociation. The inclusion of these additional pathways leads to the expression

$$\alpha = \alpha_{mie}\alpha_{cl}$$

where α_{cl} is the ratio of the rates of generation (and not of consumption of the substrate ketone) of unlabeled and labeled RPs and thus provides for an estimation of the value of α_{cl} in the photodissociation step (which is not readily accessible from a direct measurement). From the data in Table 2, α_{cl} is thus estimated to be 1.043 ± 0.012; the value for α_{cl} measured for the photodissociation of 2,4-diphenylpentan-3-one in C_{12} micelles[13a] is 1.0434 ± 0.0029 and that for dibenzyl ketone in the gas phase[18] is 1.034 ± 0.03. Thus, the differences in the values of α_{mie} and α are reasonably accounted for by the inclusion of the mass isotope effect.

Figure 2 (top) shows a plot of χ_d versus S for labeled and unlabeled MDB in both zero and high magnetic fields for all the micelles investigated; it is evident that χ_d is directly proportional to S ($\chi_d = 0.15$ S), or (from eqs 4 and 5) that $P_d/P_r = 0.15$. Thus, although the individual probabilities depend on magnetic factors, the ratio of the disproportionation probability to recombination probability is independent of the molecular and spin dynamics of the RP. This observation is wholly consistent with the assumption[15b] that the distribution of the RP amongst the different geminate reaction channels occurs *after* the completion of ISC.

We observe that $\chi_d \propto S$ also has a practical application in handling the data involving benzaldehyde. The photoinstability of benzaldehyde[16] precludes a determination of χ_d with an accuracy that is comparable to that achieved in the measurement of S. However, from the experimentally measured proportionality between χ_d and S, the value of P_d may be obtained from the correlation of Figure 2 (top) rather than from individual determinations. Also, the relatively small value of P_d ($\sim$0.1) justifies such a procedure for the evaluation of P_d.

The chemical yield χ_e of the escape products *meso*- and *d,l*-2,3-diphenylbutanes (DPB) also correlates with S (Figure 2 (bottom)), but not linearly. A qualitative explanation for this correlation may be sought in terms of a competition between the rate of escape k_e and the rate of disproportionation k_d, since $\chi_e/\delta = k_e/(k_e + k_d) = [1 - (k_d/k_r)S]$, where the ratio of k_d to k_r is a constant (as shown above) and δ is the fraction of *sec*-phenethyl radicals which react to generate DPB. Quantitatively, however, this explanation cannot be valid, since the MFE (on χ_e) = $\Delta\chi_e/\chi_e = -(k_d/k_r)\Delta S/[1 - (k_d/k_r)S] \sim -0.2$, which is inconsistent with the large MFE (ca. 90% on average) seen for χ_e (Table 1). An even more serious problem is the observation of a clear nonlinear dependence of χ_e on S (Figure 2 (bottom)). Since χ_e does not depend on the conversion of MDB (up to 70–80%), this deviation from linearity cannot be a simple consequence of the variation in the steady state concentration of the escaped *sec*-phenethyl radicals. To explain the correlation in Figure 2 (bottom), let us suppose that the benzoyl radical reacts with the detergent, with a rate constant k_s' to generate a new radical R′ (this reaction cannot be hydrogen abstraction as shown above). Also, let the *sec*-phenethyl radical react with R′ with a rate constant k_r', which is obviously spin dependent and is influenced by the magnetic field. Then, under the simplifying supposition that $k_s \gg k_e$ and $k_r' \gg k_e'$, where k_e' is the rate constant of escape of the new radical pair, it is easy to shown that

$$\frac{\chi_e}{\delta} \approx \frac{k_e'}{k_r'}\frac{k_e}{k_r}\frac{1}{S} \qquad (6)$$

This consideration explains the deviation from linearity of χ_e on S and demonstrates the possibility of a high value of the MFE on χ_e, since $\Delta\chi_e/\chi_e \sim \Delta S/S$. We note that the same argument can be applied to explain the different magnetic field dependences of different geminate products.[19]

---

(16) Gorner, H.; Kulm, H. J. *J. Phys. Chem.* **1986**, *90*, 5946.

(17) (a) Blank, B.; Henne, A.; Laroff, G. P.; Fischer, H. *Helv. Chim. Acta.* (b) Weed, G. C. Ph.D. Thesis, Columbia University, 1981.

(18) Step, E. N.; Tarasov, V. F. Unpublished results.

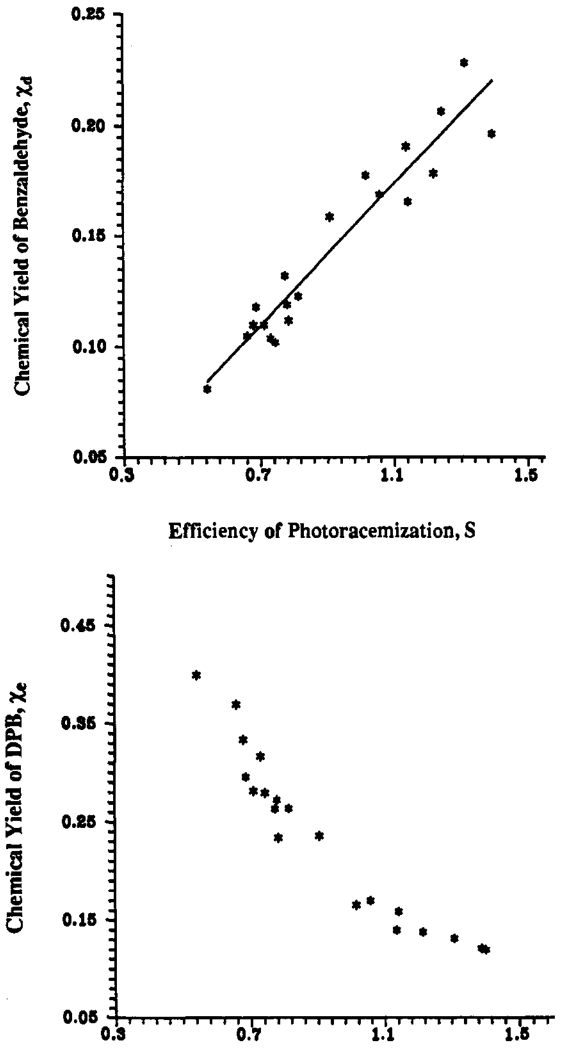

Figure 2. Correlations between the efficiency of photoracemization (S) and chemical yield of products: (top) benzaldehyde (χ_d) and (bottom) diphenylbutanes (χ_e).

Thus, all of the above considerations give us confidence in treating the experimental data in terms of eqs 2, 4, and 5 and in considering the total reaction probability of the geminate RP, $P = P_r + P_d$. The yield of *p*-ethylbenzophenone (and the corresponding probability P_{ht} in Scheme 1), produced *via* the head-to-tail coupling of the radicals, is at least 3 times smaller than that of benzaldehyde (which is ca. 0.2 on average) and is, therefore, neglected in our analysis. The value of P is measurable with high accuracy and reliability and is, therefore, a valid parameter for the computational fitting which we consider below.

Computational Models. The model of the microreactor[3,4] or supercage approximates the micelle as a spherical homogenous drop of radius L' (Scheme 2). The value of L' is assumed to depend linearly[20] on the number of carbon atoms in the detergent chain. One radical of the pair, of radius r_a, is considered fixed at the center of the micelle, while the other, of radius r_b, is allowed to diffuse. In a kinetic sense, the disadvantage of a fixed radical in the model can be avoided[3a] by the summation of the individual diffusion coefficients: $D = D_a + D_b$. The use of $D = D_a + D_b$ is valid after the "time of filling out of micelles" $Z^{-1} = V/4\pi RD$, where Z is the frequency of radical encounters, $V = 4\pi(L^3 - R^3)/3$, $L = L' - r_b$, and $R = r_a + r_b = 6$ Å. For the RP derived from MDB, is reasonable to assume that $r_a \approx r_b$ and therefore $D_a \approx D_b$. The variations in D as a function of micelle size have been discussed.[1] For the values of D used, see Table 3. One major limitation which remains is that the absolute values of D are somewhat arbitrary; however, based on literature precedent,[21] we can define a range of reasonable values of $D(C_{12})$ to be (6–16) × 10^{-7} cm^2 s^{-1}. We note that the model with surface diffusion of radicals has also been used.[3b,c,22] To the best of our knowledge there is no compelling reason to favor one kind of motion over the other.

Table 3. Values of Parameters Used in The Calculation Unless Otherwise Noted

n[a]	L (Å)[b]	D × 10^6 (cm^2 s^{-1})	σ
12	15.4	0.79	0.0432
11	14.2	1.01	0.0358
10	12.9	1.25	0.0292
9	11.6	1.49	0.0245
8	10.3	1.73	0.0206

[a] The number of carbon atoms in the detergent chain. [b] The choice of the value of L is discussed in ref 1.

To compute the reaction probability

$$P = 4\pi R^2 D\left(\frac{\partial \rho_{ss}}{\partial r}\right)_{\mathrm{R}}$$

one needs to solve the Liouville equation for the time integrated density matrix of the RP spin system[12]

$$\frac{D}{r}\frac{\partial^2(r\rho(r))}{\partial r^2} - \mathbf{L}\rho(r) - \mathbf{R}\rho(r) - \mathbf{K}\rho(r) = -\left[\frac{\delta(r-R)}{4\pi R r_0}\right] \tag{7}$$

The RP is assumed to be generated in the contact state ($r_0 = R$) at $t = 0$.

The spin selective reaction operator[23] **K** for the Liouville equation is given by eq 8, where k_s may be considered as the reaction rate constant

$$\mathbf{K}\rho = {}^1/_2 k_s[\mathbf{P}_s\rho + \rho\mathbf{P}_s] \tag{8}$$

of the singlet radical pair in the reaction zone Δ.[12c] In performing the calculations, neither k_s nor Δ was used in an explicit form; rather, the dimensionless parameter $k_s\Delta R/D = k_s\tau$ was used to characterize the reaction ability of the RP for actual calculations. $\mathbf{P}_s$ is the projection operator into the singlet spin manifold.

The external boundary condition[1] (eq 9; see also for ref 4a) models the escape of the radicals through the boundary to the bulk aqueous phase, and σ is a dimensionless boundary factor which is related to the inherent probability of escape when the radical reaches the boundary.

$$\frac{\partial \rho}{\partial r}\Big|_{r=L} = -\frac{\sigma}{L}\rho\Big|_{r=L} \tag{9}$$

Some quantitative conclusions can be drawn from a consideration of RP spin nonselective reactions after the time of filling out of the micelle. For the case of diffusion limited travel across the boundary[27]

$$k_e = \left(\frac{3D_w}{L^2}\right)\exp\left(\frac{\Delta G_m{}^\circ}{RT}\right) \tag{10}$$

where $\Delta G_m{}^\circ$ is the difference in free energies of radicals (assumed to be the same for both radicals) in the micelle interior and in the bulk water. D_w is the diffusion coefficient of radicals just outside the boundary, which

---

(19) Step, E. N.; Buchachenko, A. L.; Turro, N. J. *Chem. Phys.* **1992**, *162*, 189.

(20) (a) Borbely, S.; Cser, L.; Ostamvich, Y. M.; Vass, S. *J. Phys. Chem.* **1989**, *93*, 7967. (b) Tanford, C. *The Hydrophobic Effect*; John Wiley: New York, 1980. (c) Tanford, C. *J. Phys. Chem.* **1972**, *76*, 3020.

(21) (a) Turley, W. D.; Offen, H. W. *J. Phys. Chem.* **1985**, *89*, 2933. (b) Turro, N. J.; Aikawa, M.; Yekta, A. *J. Am. Chem. Soc.* **1979**, *101*, 772. (c) Zachariasse, H. A. *Chem. Phys. Lett.* **1978**, *57*, 429. (d) Turro, N. J.; Okubo, T. *J. Am. Chem. Soc.* **1981**, *103*, 7224. (e) Emert, J.; Behrens, C.; Goldenberg, H. *J. Am. Chem. Soc.* **1979**, *101*, 771. (f) Grieser, F.; Drummond, C. J. *J. Phys. Chem.* **1988**, *92*, 5580.

(22) Hore, P. J.; Hunter, D. A. *Mol. Phys.* **1992**, *75*, 1401.

(23) We used another form of the reaction operator $K = k_s\langle P_s\rho P_s\rangle$ in our previous papers (refs 1, 4d, and 24). This operator has been criticized (ref 25). Note that this operator has been successfully used in many applications (refs 24 and 26). We will discuss in detail the differences between the two operators in our next publication.

(24) (a) Shkrob, I. A.; Tarasov, V. F.; Bagryanskaya, E. G. *Chem. Phys.* **1991**, *153*, 427. (b) Bagryanskaya, E. G.; Tarasov, V. F.; Avdievich, N. I.; Shkrob, I. A. *Chem. Phys.* **1992**, *162*, 213.

(25) Haberkorn, R. *Mol. Phys.* **1976**, *32*, 135.

(26) (a) Batchelor, S. N.; McLauchlan, K. A.; Shkrob, I. A. *Mol. Phys.* **1992**, *75*, 501. (b) Batchelor, S. N.; McLauchlan, K. A.; Shkrob, I. A. *Mol. Phys.* **1992**, *75*, 531.

(27) Almgren, M.; Greiser, F.; Thomas, J. K. *J. Am. Chem. Soc.* **1979**, *101*, 279.

Scheme 2. Model of the Microreactor

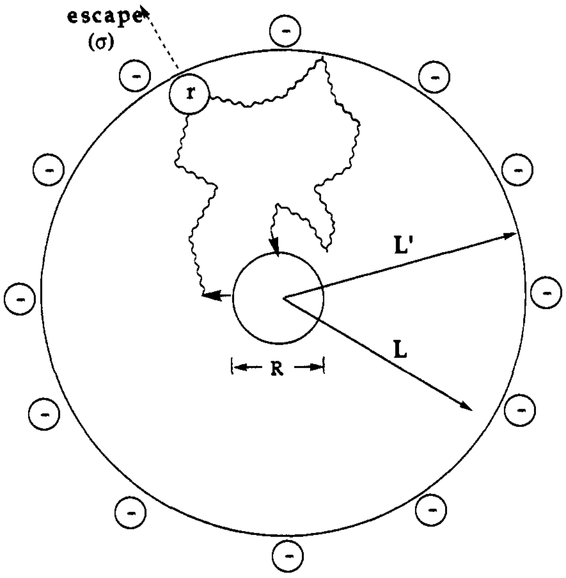

Assumptions and Definitions

1) Micelle is considered as a spherical homogeneous drop

2) Escape of radical from micelle is considered to be irreversible

3) R = 2r = radius of reaction sphere

4) L = radius of free volume

5) D = Coefficient of mutual diffusion

6) σ = Boundary factor

may be approximated to that in bulk water. It follows from eq 9 that

$$\sigma = \left(\frac{D_w}{D}\right)\exp\left(\frac{\Delta G_m{}^\circ}{RT}\right) \qquad (11)$$

or

$$k_e = \frac{4\pi RD}{V}\,\frac{\sigma}{1-\sigma}\,\frac{L}{R} \approx \frac{3D}{L^2}\sigma \qquad (12)$$

Note that a calculation of the escape rate, k_e, performed under the approximation that $\Delta G_m{}^\circ$ is invariant with micelle size gives results which are very close to experimental,[24d,28] ones. The values of σ used are given in Table 3.

The superoperator L is given by eq 13, where k' is the rate constant of spin nonselective scavenging reactions of the radicals. In our calculations we use $k' = 1 \times 10^5$ s^{-1}. H is the effective spin Hamiltonian of the RP. We consider two models: in model I H is given by

$$\mathrm{L} = i[\mathrm{H}\rho - \rho\mathrm{H}] - k'\rho \qquad (13)$$

$$\mathrm{H} = \sum A^a{}_i S_a I_i + \sum A^b{}_j S_b I_j - J(r)(2S_aS_b + {}^1/_2) \qquad (14)$$

while in model II

$$\mathrm{H} = A^* S_a I_a + \sum A^b{}_j S_b I_j - J(r)(2S_aS_b + {}^1/_2) \qquad (15)$$

where A^* refers to the ^{13}C nucleus and subscript a refers to the benzoyl radicals, while subscript b refers to the pertinent nuclear spins in the *sec*-phenethyl radical. Because of computational limitations, we consider only four nuclei in model I (three H_β and one H_α for the unlabeled RP; three H_β and one ^{13}C for the labeled pair).

In both models J is given by eq 16, where J_0 is the average ESE in the contact state at $r = R$. The assumed value of $\lambda = 5 \times 10^{-9}$ cm is very similar to that used by others.[12a,b] All calculations in this paper have been performed with $J_0 = 13 \times 10^9$ rad s^{-1}.[1]

$$J(r) = J_0 \exp[-(r-R)/\lambda] \qquad (16)$$

Paramagnetic relaxation is described by the operator R in model II and is considered[29] in the Redfield approach. Paramagnetic relaxation is ignored in model I. However, model I assumes that the spin level population in the RP is equilibrated at time $t = 0$; no such assumption is made for model II, where the RP is considered to be in the triplet state at $t = 0$.

In comparing the experimental and theoretical values of the reaction probability, it is important that the models do not distinguish between the different chemical channels of possible geminate reactions: recombination, disproportionation, or head-to-tail coupling (Scheme 1). The theory calculates $P = P_r + P_d + P_{ht}$ as the total reaction probability of the RP and assumes that the products distribute among the reaction channels after the completion of ISC. The theory is inapplicable if this condition is not fulfilled. We note that support is provided by the observed independence of the S/χ_d ratio on the magnetic field and HFI (Figure 2 (top)) and a reported rigorous analysis of the isotope content in benzaldehyde.[30]

Discussion

The observations of a typical HFI mechanism of the magnetic field effect (MFE)[4d,15] and a significant MIE involving the micellized RP from MDB support the hypothesis that the HFI provides a decisive contribution to ISC in the systems investigated. In the first paper in this series,[1] we concluded that ESE modulated ISC, induced by the HFI, limits the rate of unlabeled geminate RP recombination in small micelles. At this point we seek to resolve the following issues: (1) What is the mechanism of the limitation and how is the limitation manifested in the dependence of reaction probability on micelle size? (2) What role, if any, does paramagnetic relaxation play in the ISC of the RP considered? (3) How is paramagnetic relaxation manifested in the dependence of the reaction probability on micelle size?

In order to the answer the first question, we examine the simple example of a RP possessing a single magnetic nucleus with the HFI constant, A. Since $\sigma L/R < 0.1$, the exponential model can be applied to RP decay with $k \approx Zk_s\tau/(1 + k_s\tau)$ as the rate constant of a singlet RP reaction. For the purpose of qualitative considerations, we use an effective ESE described by J_{eff}. We now define r^* as $J(r^*) = A$, and we do not consider the unrealistic case involving an ESE so strong that $r^* \gg L$; stated differently, the condition $r^* < L$ means that even for the smallest micelles the RP can achieve separations large enough so that the exchange interaction is negligible relative to the hyperfine interaction. The corresponding problem with the spin selective reaction operator in the form of eq 8 can be solved analytically. For example, for $B_0 = 0$ and $k_s\tau \gg 1$ (so that $f = k_e/k = \sigma L/R \ll 1$), the value of P is given in eq 17, where $G = A^2 + 2AJ_{\mathrm{eff}} + 4J_{\mathrm{eff}}{}^2$.

$$P = A^2/[3A^2 + 4f(k^2 + 4G)] \qquad (17)$$

We initially consider the case where we can neglect ESE ($J_{\mathrm{eff}} = 0$). Then from eq 17 it follows immediately that, as a function

---

(28) (a) Evans, C. H.; Scaiano, J. C.; Ingold, K. U. *J. Am. Chem. Soc.* **1992**, *114*, 140. (b) Levin, P. P.; Kuzmin, V. A. *Chem. Phys.* **1992**, *162*, 79.

(29) (a) Koptyug, I. V.; Lukzen, N. N.; Bagryanskya, E. G.; Doktorov, A. B.; Sagdeev, R. Z. *Chem. Phys.* **1992**, *162*, 165. (b) deKanter, F. J. J.; den Hollander, J. A.; Huizer, A. H.; Kaptein, R. *Mol. Phys.* **1977**, *34*, 857.

(30) Step, E. N.; Buchachenko, A. L.; Turro, N. J. *Chem. Phys. Lett.* **1991**, *186*, 405.

of L, P passes through a maximum at the point $L_{max}^3 = (5)^{1/2}3RD/A$ (k and f are functions of L). P is inversely proportional to L as along as $A/Z \gg 1$. This is the same result predicted by a mechanical analysis alone.

However, when $A/Z \ll 1$, the value of P decreases rapidly as L^5 according to eq 17. A comparison of eq 17 with the simple monoexponential kinetic result $P = k_r/(k_r + k_e)$ shows that $k_r \approx (A^2/Z^2)Z$. This means that in this limit of $A/Z \ll 1$ *the faster the rate of encounters, the slower the rate of geminate recombination.* This result is strikingly nonintuitive because the exchange interaction is explicitly considered to be zero, and based on the classical cage effect (without spin), the faster reencounters would be expected to compete better with diffusional escape and therefore increase the rate of geminate recombination. We now introduce the parameter $Z^* = 3r^*D/(L^3 - R^3)$, which is the frequency of radical encounters within an imaginary sphere of radius r^* ($J(r^*) = A$). If $A/Z^* \gg 1$, we can neglect the influence of the ESE on the reaction ability of the RP since ISC is not rate determining. Then the influence of ESE is not critical in determining the reaction ability of the RP and will simply be held to the extent of the appearance of the target parameter (R/r^*) in the formula for $k_r \sim (R/r^*)Z^*/4$ and again the mechanical prediction remains valid. If $A/Z^* \ll 1$, we can introduce J_{eff} as a result of the averaging of the ESE along the diffusional trajectories by eq 18, where $\mu = J_0\lambda R/D$ characterizes the

$$J_{eff} = 3J_0\lambda R^2/(L^3 - R^3) = \mu Z \qquad (18)$$

efficiency of the electron exchange event per forced encounter. The probability of recombination as a function of L still exhibits a maximum, but ESE shifts the L_{max} to the range of larger L, since $L_{max}^3 = [(5)^{1/2} + 2\mu]3RD/A$ (eq 17) for $\mu \ll 1$ and $L_{max}^3 \approx 7\mu RD/A$ for $\mu \gg 1$. The condition of negligible ESE means now that $\mu \ll A/Z^* \ll 1$. This is a much stronger constraint than the usual definition of weak exchange $\mu \ll 1$.[31] Note that the value of μ is limited by the condition that $J_{eff} < J_0$.

Figure 3 shows the results of the computer solution of eq 7 for the hypothetical mononuclear RP. To focus on the influence of the spin dynamic parameters, we have calculated P for the case of a totally reflecting boundary ($\sigma = 0$) and for homogeneous radical escape with $k_e' = 5 \times 10^6$ s^{-1}. It is seen in Figure 3 that the conclusions drawn above from simple physical considerations are qualitatively reproduced by the solution of the Liouville equation: increasing the value of A (Figure 3 (top left)) and decreasing the value of D (Figure 3 (top right)) and the value of J_0 (Figure 3 (bottom left)) lead to a shift in the maximum of the P curves toward a smaller L.

The above discussion was carried out for the condition of a fast reaction in the reaction zone. For the condition of a slow reaction in the reaction zone, $k_s\tau \ll 1$, we should replace the frequency of forced encounters, Z, by the frequency of reactive encounters, $k_s\tau Z$ (for $k_s\tau \ll 1$, but $k_s\tau Z \gg k_e$). The result of this is that the smaller the value of $k_s\tau$, the smaller the value of L_{max} (see Figure 3 (bottom right)).

Our considerations are based on the solution of the Liouville equation for the system enclosed in a supercage with a partially reflecting boundary. Analysis of the Liouville equation for the two-site model of the microreactor has been presented recently;[32] however, this analysis is primarily devoted to the effect of ESE and chemical reactivity of the RP on its ESR spectra. These publications[32] were the first instances where the peculiarities of the reaction operator as given by eq 8 have been discussed.

Figure 4 pictorially summarizes the discussion presented above. A simple mechanical[1] analysis of the system of a micellized RP leads to the conclusion that the probability of recombination should increase as the micelle size decreases. However, an analysis which concurrently considers hyperfine and exchange interactions along with the mechanical factors shows that the dependence of P on L actually has a maximum. The value of L_{max} (Figure 4) increases as A decreases, as D increases, and as J increases. The parameter A_{eff}/Z (A_{eff} defines the frequency of the ISC transitions in a multinuclear RP) is critical in determining whether P increases or decreases as L changes: If $A_{eff}/Z \gg 1$, then the dependence of the cage effect on the micelle size could be predicted by a mechanical analysis[1] of $f = k_e/k \sim k_e/Z$ ratio (Figure 4); in this instance one can neglect the influence of ESE, i.e. the rate of reencounters is slower and rate determining. If, on the other hand, $A_{eff}/Z \ll 1$, then ISC is slower and rate determining, and the supercage effect as a function of the microreactor size will demonstrate the behavior opposite to that predicted by a simple mechanical analysis; in this case it is impossible to neglect ESE for low reactive singlet contact RPs (small $k_s\tau$). The important conclusion of the model then is that *the significance of ESE in determining the rate of recombination reactions in the supercage is determined by the rate of ISC due to A_{eff}* ***relative*** *to the rate of reencounters: the smaller the ratio of A_{eff}/Z the greater the role played by the exchange interaction.*

We now model a more realistic situation. **Model I.** To fit the experimental results, we use a boundary factor $\sigma \sim 0.04$–0.02 (Table 3). The variation in σ is employed to account for the expected variation in D with L (eq 12), and furthermore, this reproduces the experimental values of k_e.[28] Since the largest value of L is ~15.4 Å and $R = 6$ Å, we have $f = k_e/k \approx 0.1$–0.05. From these parameters, the ratio of A_{eff}/Z is ~1.2 ($A_{eff} \approx 30$ G[12b]) in C_8 micelles and ~12 in C_{12} micelles. Thus, the turnover point (L_{max}, Figure 4), when only processes induced by HFI in nonlabeled RPs are considered, is expected to occur for the smallest micelles, i.e. C_8 and C_9 micelles, and P_r *should* decrease with increasing size on going from C_8 to C_{12}. However, introducing ESE into the consideration (for the values of J_0 used, $\mu \approx 5$) causes the turnover point to shift to the range of ~16 Å and the opposite behavior of P_r is seen. The fact that model I reproduces the experimental observations quite well (Figure 5 (top)) with the *nonlabeled pair* in both zero and strong magnetic fields justifies that the effects of both forced encounters and ESE are important for the nonlabeled RP. Nevertheless, from the above considerations, we can neglect the influence of ESE on the absolute value of P in large (C_{11} and C_{12}) micelles.

However, model I fails when applied to the labeled RP* (Figure 5 (bottom)). For the RP*, $A^*_{eff}/Z > 4$ even for the C_8 micelle. To shift the turnover point to the range of C_{11} and C_{12} micelles, one would require such small values of $k_s\tau$ and such large values of J_0 that the theoretical values of P become negligibly small in comparison with the experimental ones. Another arbitrary approximation of model I is that of equilibrated spin level populations at the time of RP creation. Therefore, we consider the computational results from model II, which can obviously only be applied to the labeled RP, and answer the second question asked above concerning the role of paramagnetic relaxation.

Model II, Strong Magnetic Field. Initially we would like to determine whether one can neglect the electron–electron dipole–dipole interaction (DDI) induced paramagnetic relaxation on the dependence of P on L. We consider three different modes to account for the paramagnetic relaxation due to DDI. The first of these is based on the model by Hayashi.[34] In this approach, the radicals are considered to relax at some distance r with a rate defined by rotational motion of the micelle with the correlation time $\tau_m = 3kT/4\pi\eta L^3 > 2 \times 10^{-9}$ s, where η is the viscosity of water ($\approx 0.8 \times 10^{-2}$ P). The second approach arises from an

---

[31] Shushin, A. I. *Chem. Phys. Lett.* **1990**, *170*, 78.

[32] (a) Shushin, A. I. *Chem. Phys. Lett.* **1991**, *181*, 274. (b) Koptyug, I. V.; Lukzen, N. N.; Bagrayanskaya, E. G.; Doctorov, A. B. *Chem. Phys. Lett.* **1990**, *175*, 467.

[33] Atherton, N. M.; Strach, S. J. *J. Chem. Soc., Faraday Trans. 2* **1972**, 374.

[34] Hayashi, H. *Bull. Chem. Soc. Jpn.* **1984**, *57*, 1753.

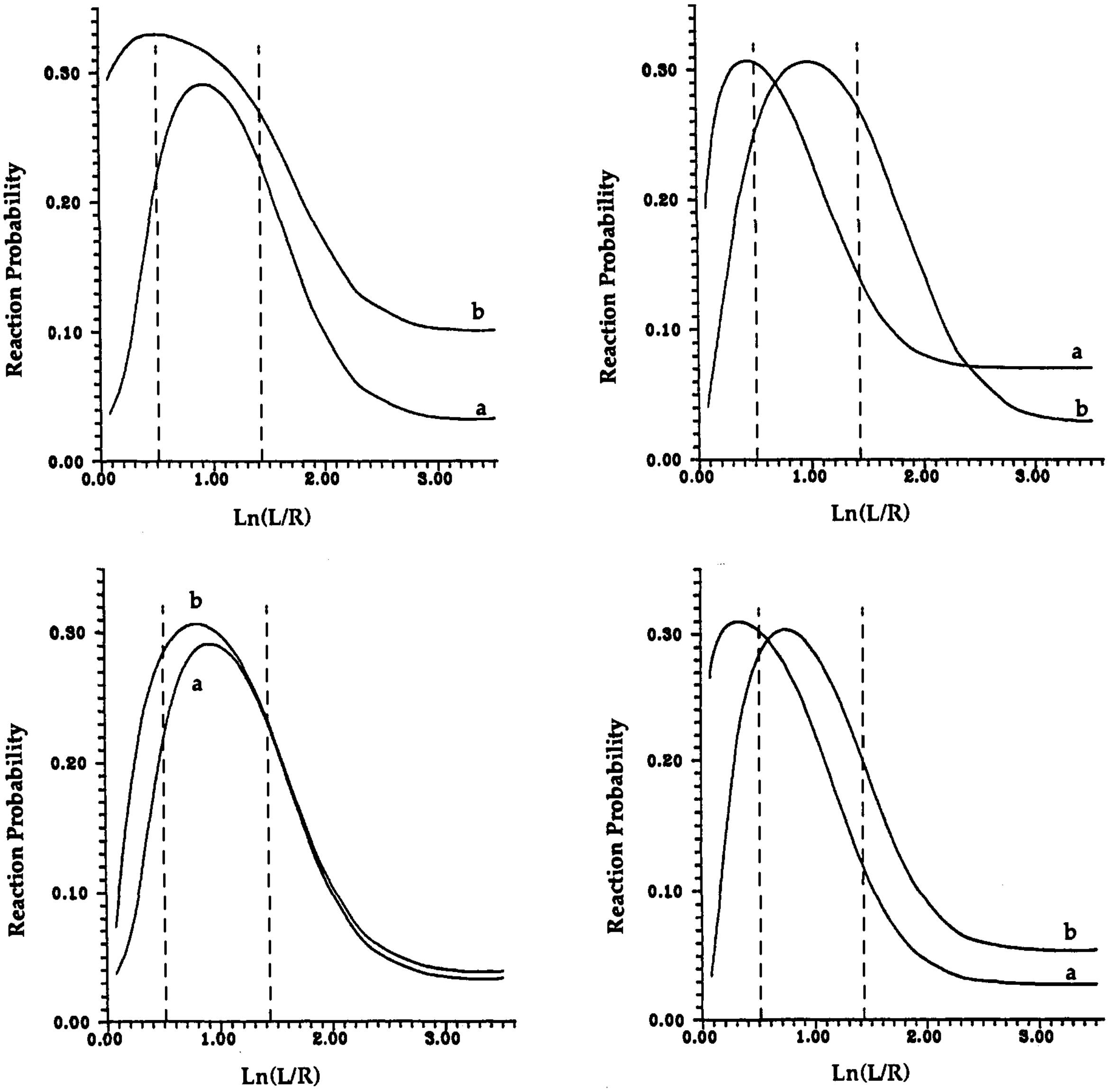

Figure 3. Modulation of the supercage effects as a function of the supercage size due to parameters affecting molecular, diffusional, and spin dynamics of the radical pair: (top left) $J_0 = 2 \times 10^{11}$ rad/s, $D = 2 \times 10^{-6}$ cm²/s, $k_s\tau = 8$, $A = -16.3$ G (curve a), $A = 124$ G (curve b); (top right) $J_0 = 0$, $k_s\tau = 8$, $D = 4 \times 10^{-6}$ cm²/s (curve a), $D = 4 \times 10^{-7}$ cm²/s (curve b), $A = -16.3$ G; (bottom left) $J_0 = 0$ (curve b), $J_0 = 2 \times 10^{11}$ rad/s (curve a), $D = 2 \times 10^{-6}$ cm²/s, $A = -16.3$ G, $k_s\tau = 8$; (bottom right) $J_0 = 0$, $D = 2 \times 10^{-6}$ cm²/s, $A = -16.3$ G, $k_s\tau = 8$ (curve a), $k_s\tau = 64$ (curve b); $\sigma = 0$ for all cases (see text); dashed lines show the available experimental range of the variation in the L/R ratio.

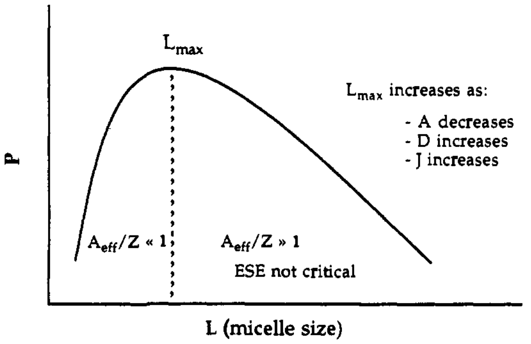

Figure 4. General features of the dependence of P on L. See text for details.

attempt to take into account the fact that PhCO• is a σ radical. If one assumes that the angle $\pi R/L$ is large enough to induce relaxation, then the rotation of σ radicals should be considered since it is much faster than the rotation of micelles. This is approximately achieved by using the rotational correlation time τ_c of the radical itself. The value of $\tau_c = 30$ ps/rad was used for C_{12} micelles since the rotational correlation time of small stable nitroxide radicals in C_{12} micelles lies in this range.[33] The relative variations in τ_c with L were defined by the dependence of the rotational correlation time of a stable nitroxide[1] on L. This approach is consistent with the requirement of short correlation times which had been invoked[15b] to fit the magnetic field dependence of P_r in C_{12} micelles. Both the Hayashi approach and the second approach actually take into account the orientational relaxation of the vector connecting the two dipoles. DDI relaxation induced by the translational motion of radicals in micelles can be described in terms of an approach recently outlined by Steiner.[35] According to this approach, the $T_0T_\pm$ relaxation due to DDI modulated by translational diffusion can be described by two correlation times that actually are expressed through the translational diffusion coefficient, D. In this treatment, the rotational motion of the micelle is not taken into account and the rotational motion of radicals themselves (both of which are considered to be π radicals) is considered to be unimportant.

For an estimation of the relaxation rate R_{DDI} of the $T_\pm T_0$ sublevels due to translational motion of the radical, we can compare Steiner's data with an equation analogus to that for ESE (eq 18) and easily find that, in our case for $B_0 = 2400$ G,

---

(35) Steiner, U. E.; Wu, J. Q. *Chem. Phys.* **1992**, *162*, 53.

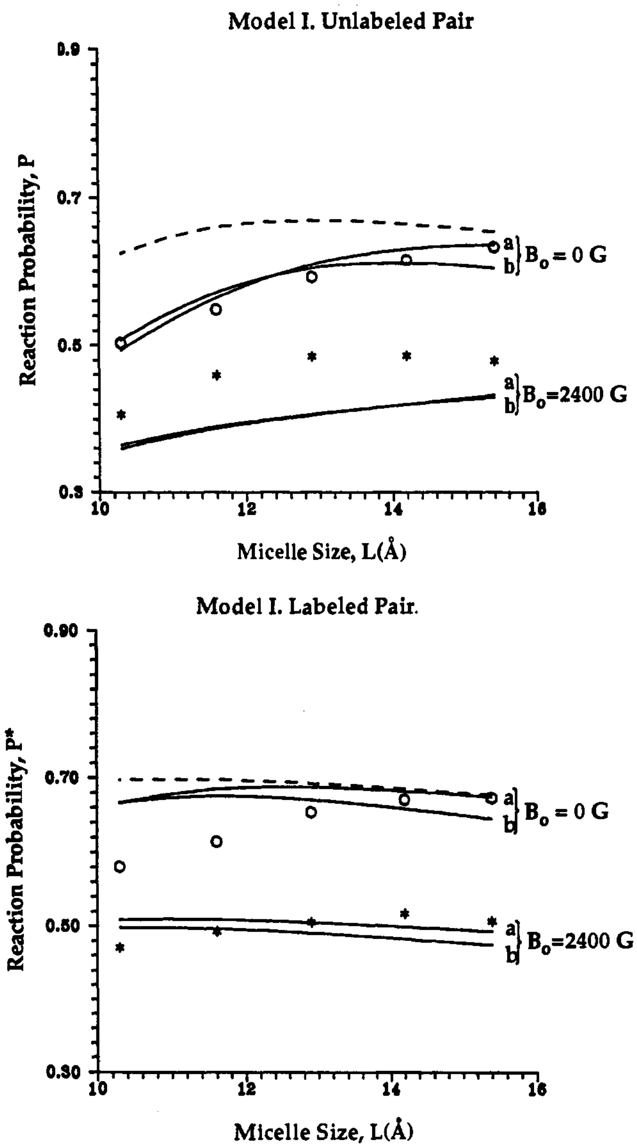

Figure 5. Fitting of the experimental results in the frame of model I: (top) unlabeled RP and (bottom) labeled RP. For a curves, $D(C_{12})$ = 1.34×10^{-6} cm²/s, and for b curves, $D(C_{12}) = 0.79 \times 10^{-6}$ cm²/s. Dashed curves are calculated for $J_0 = 0$ ($B_0 = 0$) with the same parameters as for the b curves. All other parameters are described in the text.

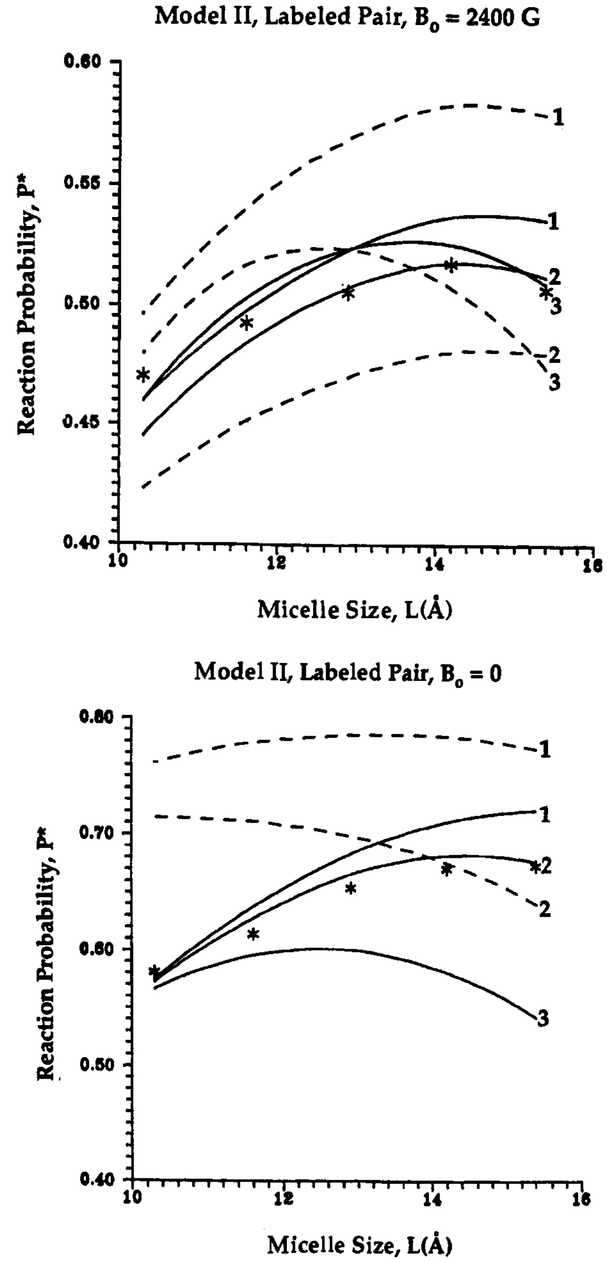

Figure 6. Fitting of the experimental results in the frame of model II. (top) B_0 = 2400 G. Solid lines: $k_s\tau = 8$, $[A{:}A] = 1.06 \times 10^{17}$ rad²/s² (curve 1); $k_s\tau = 4$, $[A{:}A] = 1.06 \times 10^{17}$ rad²/s² (curve 2); $k_s\tau = 2$, $[A{:}A]$ = 1.58×10^{17} rad²/s² (curve 3). Dashed lines: $k_s\tau = 8$, $[A{:}A]$ = 1.58×10^{17} rad²/s² (curve 1); $k_s\tau = 8$, $[A{:}A] = 6.18 \times 10^{16}$ rad²/s² (curve 2); $k_s\tau = 1$, $[A{:}A] = 2.62 \times 10^{17}$ rad²s/² (curve 3). (bottom) $B_0 = 0$ G. Solid lines: $k_s\tau = 32$, $[A{:}A] = 6.18 \times 10^{16}$ rad²/s² (curve 1); $k_s\tau = 4$, $[A{:}A] = 1.06 \times 10^{17}$ rad²/s² (curve 2); $k_s\tau = 2$, $[A{:}A] = 2.62 \times 10^{17}$ rad²/s² (curve 3). Dashed lines: H_{aniso} is neglected, and DDI is taken into account in the frame of the Steiner[35] approach; $k_s\tau = 32$ (curve 1), $k_s\tau = 2$ (curve 2). The value of all other parameters are given in the text.

$R_{\mathrm{DDI}} \leq 5 \times 10^5$ s^{-1}, mostly because of the small probability of DDI induced transitions per forced encounter. To estimate R_{DDI} in a second approach, one may introduce the average distance between radicals as $(RL)^{1/2}$ = 9.6–7.9 Å in C_{12}–C_8 micelles. The variation in τ_c with micelle size is unimportant, since $\gamma_e B_0 \tau_c \approx 1.3$. Thus, $R_{\mathrm{DDI}} \leq 5 \times 10^5$ s^{-1}, which is much smaller than the observed rate of decay of the RP and hence unimportant.

In the frame of Hayashi's approach, the average distance between radicals should be replaced by the micelle size L'. In this case, $\gamma_e B_0 \tau_m \approx 13$ and we find almost the same value for R_{DDI}. Thus, we may expect that it is only the anisotropic HFI induced paramagnetic relaxation which influences the dependence of P on L in a strong magnetic field.

The rate of paramagnetic relaxation due to HFI$_{\mathrm{aniso}}$ is defined by τ_c and the inner product of the HFI tensor with itself $[A{:}A]^{1/2}$, the value of which is not known for the benzoyl radical. So actually two parameters are still arbitrary, $[A{:}A]$ and $k_s\tau$ (as it follows from our previous estimation, the P^* value shows a weak dependence on ESE in labeled RP*, since $A/Z \gg 1$). The slope of the $P^*(L)$ dependence is almost insensitive to the $[A{:}A]$ value (compare curves 1 and 2 (dashed) with 1 and 2 (solid) in Figure 6 (top)). This allows us to find $[A{:}A] = 6 \times 10^{16}$ to 6×10^{17} rad²/s² and $k_s\tau$ = 4–8 as a good range of parameters (see solid curves in Figure 6 (top)). Note that for the $H^{13}CO$ radical $[A{:}A]$ = 3.1×10^{17} rad/s,[6b] so the value of $[A{:}A]$ used is reasonable. Thus we see that, for the labeled pair in a strong magnetic field, predictions close to experimental results are only possible when relaxation due to anisotropic HFI are considered.

Model II, Zero Magnetic Field. There is no reason for local fields in the zero magnetic field[36] if the uncoupled electrons of radicals of RP do not interact with each other, but the uncoupled electrons are involved in DDI. In this context, we tentatively

---

[36] Okazaki, M.; Tai, Y.; Nunome, K.; Toriyama, K.; Nagakura, S. *Chem. Phys.* **1992**, *161*, 177.

assume that the calculation of the relaxation matrix R for eq 7 can be applied to the case of zero field, but with the same correlation (shortest) time for both HFI_{aniso} and DDI. This seems to be a good approximation, since the theoretical curves with the parameters defined from fitting the high-field experiment reproduce the experimental curves in zero magnetic field reasonably well (solid curve 2 in Figure 6 (bottom)). Note that computational results show low sensitivity to the value of τ in the range 30–60 ps, but any attempts to reproduce the experimental results using $\tau_c > 10^{-10}$ s fail even qualitatively.

Unlike the case for strong magnetic fields, R_{DDI} cannot be neglected in either the Hayashi[34] or the Steiner[35] approach in low magnetic fields. Hayashi's approach predicts a substantial monotonic increase in P with decreasing micelle size, and this is contrary to the experimental observations.[37] Thus the Hayashi approach,[34] which gives an excellent description of ISC in RPs formed due to photoreduction in micelles (one of the radicals resides on the detergent chain), is inappropriate for our case. There appears to be little correlation between diffusional motion of relatively small radicals and the rotational motion of the micelle itself.

Consideration of relaxation due to anisotropic HFI and DDI in the Steiner approach in zero magnetic field demands that the mutual orientation of the radicals and the distance between them be taken into account; this is a considerable computation problem for even the simplest RP. Therefore, to demonstrate the importance of DDI in zero magnetic field, we calculated the dependence of P^* on L in the Steiner approach neglecting HFI_{aniso} (see dashed curves 1 and 2 in Figure 6 (bottom)). The lack of a good fit suggests that DDI alone cannot explain the experimental dependence of P^* on L in zero magnetic field.

The reasonable fit of the experimental results in the framework of model II indicates that the suggestion of equilibrated spin state population at $t = 0$ is not necessary if paramagnetic relaxation is included in the computation. The uncoupled electrons in the nonlabeled RP experience the same DDI as do those in RP*. In this sense it is clear that the successful fit of experimental data of P (model I) is most likely a consequence of a compensation between a decrease in the rate of paramagnetic relaxation due to HFI_{aniso} and an increase in the rate of paramagnetic relaxation due to DDI with a decrease in micelle size in a small magnetic field. In addition, there is a negligible contribution of paramagnetic relaxation in the L dependence of P in a strong magnetic field since the rate of paramagnetic relaxation due to anisotropic HFI in nonlabeled RPs is at least one order smaller than that which exists in the labeled pair.

Besides discussing the effects of micelle size on P_r and P_r^* in zero and high magnetic fields, the variation in MFE as a function of micelle size is also an interesting question that may be considered. However, this will be the subject of future considerations.[38]

Our analysis shows that microrestriction of the diffusional motion of the geminate radical pair provided by the micellar supercage leads to several important features of spin selective chemical reactions of the geminate pair when they are conducted within the supercage. The first feature is the possibility of retardation of the HFI induced ISC by the frequent forced encounters; this effect is most pronounced in small nonviscous micelles with RPs possessing small HFI. The second feature is the retardation of ISC due to ESE between uncoupled electrons. Retardation of ISC due to forced encounters and due to ESE is important under the same conditions; an increase in reactivity of contact singlet RPs ($k_s\tau$) diminishes the importance of ESE in this retardation, and in turn, the decrease in $k_s\tau$ diminishes the importance of fast forced encounters. The third feature is the influence of paramagnetic relaxation, which is most pronounced for reactions in large micelles. It is not possible at this time to state which effect is most important in the case being considered here, since the variations in micelle size, viscosity, and HFI actually fulfill the marginal condition $A_{eff}/Z \sim 1$ (see Figure 3 for an example).

However, it is clear is that the influence of ESE on the reaction ability of the labeled RP* can be neglected for all the micelles. Furthermore, the contribution of paramagnetic relaxation due to anisotropic HFI for the RP* cannot be ignored in strong magnetic fields in the dependence of P^* on L. Finally, ESE along with retardation due to the A/Z factor cannot be neglected for unlabeled RPs especially in small micelles; but relaxation does not seem to be important in the dependence of P on L.

Magnetic Isotope Effect. The early interpretation of the magnetic isotope effect (MIE) and the separation of isotopes due to the MIE[4b,7] was based on definite reasoning, i.e. the higher the value of HFI, the higher the rate of ISC, the faster the rate of recombination in a triplet born RP, and the higher the enrichment efficiency of the substrate ketone in the isotope possessing the additional HFI. It was expected that, in micellar media, the higher the HFI the higher the value of P. However, a simple comparison of the observed lifetime of the RP in the micelle with the HFI induced rate of ISC neglecting other processes shows[9] that this logic is incomplete. Even for the case of the unlabeled RP from MDB, the rate of ISC according to quasiclassical estimations should be $\sim 2 \times 10^8$ s^{-1}, which exceeds the inverse of the lifetime of the micellized RP, $\sim 10^7$ s^{-1}. Thus, the HFI mechanism of ISC cannot be rate limiting for the reaction of the geminate pair. An identical argument is also valid for the classic example of dibenzyl ketone.[7] We are therefore led to the interesting conclusion that the *an increase in HFI from the magnetic isotope may not generally increase the rate of recombination of a geminate radical pair in a restricted reaction space such as a supercage*. Furthermore, simple reasoning based on the suggestion that HFI is the single source of ISC in the RP predicts[1] an increase in the probability of geminate reactions with decreasing L (micelle size) in the RP under consideration, which is contrary to our observations (Table 2).

On the basis of the assumption that HFI was the "sole source" determining ISC, a small reaction ability ($k_s\tau \ll 1$) between the benzyl and acyl termini of biradicals derived from α-methylcycloalkanones was suggested[39] in order to explain the low efficiency observed in isotope separation for this reaction. Now it is clear that this "small" reaction efficiency is probably due to the very fast encounters of the termini of biradicals (in a nonviscous medium) and to a very high reaction ability of the termini in the singlet state. For such systems, the rate of ISC is suppressed by both encounters and ESE, leading to a small probability of reaction of the termini. As a result $\alpha \to 1$, i.e. there is a small or negligible efficiency of isotope separation. Nevertheless, a large isotope separation efficiency was found in the side products[40] of biradical reactions since these products are not constrained by the geminate reaction probability but by the ratio of the corresponding rate constants of product formation which is defined by the ratio of A^{*2}/A^2 which is still high.

The value of α in large micelles is defined mostly by the recombination events which occur before the time of filling out or a "local cage in a supercage" effect. This is the reason why α in C_{12} micelles for DPP, which gives rise to short lived RPs ($\sim$20 ns), is almost the same as in the RP derived from MDB despite a large difference in the geminate reaction probability, i.e., *the local cage effect dominates*.[13a] However, in the case of MDB, the filling is complete during the longer RP lifetime so that, when the micelle size decreases, the effects both of retardation

---

(37) Tarasov, V. F.; Ghatlia, N. D.; Avdievich, N. I.; Turro, N. J. *Z. Phys. Chem.*, in press.

(38) Tarasov, V. F.; Ghatlia, N. D.; Bagryanskaya, E. G.; Turro, N. J. Manuscript in preparation.

(39) Klimenok, B. B.; Tarasov, V. F.; Buchachenko, A. L. *Bull. Acad. Sci. USSR, Div. Chem. Sci.* (*Engl. Transl.*) **1984**, *33*, 1072.

(40) Turro, N. J.; Doubleday, C.; Hwang, K.; Cheng, C.; Fehlner, J. R. *Tetrahedron Lett.* **1987**, *28*, 2929.

in ISC due to rapid encounters and of ESE are mostly pronounced in the nonlabeled RPs. This provides an answer to the question of why the value of α increases when the micelle size decreases despite the fact that the germinate reaction probability decreases: the value of P_r, which is much more susceptible to the changes in the magnetokinetic environment induced by decreasing the micelle size, diminishes more rapidly than does P_r^*, which is buffered from these changes by the large HFI. Finally, the rapid rate of increase in α with decreasing L as predicted by model I is not realized experimentally since model I neglects paramagnetic relaxation, which provides an additional source of ISC in the labeled RP, the contribution of which decreases with micelle size.

Conclusions

In this study we have extended the systematic investigation of micelle size effects on the reactivity of geminate radical pairs solubilized in alkyl sulfate micelles of varying sizes (C_8–C_{12}), employing the magnetic labeling of the pair as a probe and magnetic isotope separation efficiency as an observable parameter. The probabilities of recombination and disproportionation of two radical pairs differing only in their HFI (^{13}C *versus* ^{12}C at the carbonyl carbon) were measured in zero and high magnetic fields. Despite the fact that the geminate pair reaction probability monotonically decreases with decreasing micelle size in both zero and high fields, it was observed that the isotope separation efficiency, in zero magnetic field, increased as the size of the supercage decreased. This effect was established using a direct isotopic measurement of α as well as from the independent measurements of the probabilities of recombination. The magnetic field effect for both labeled and unlabeled RPs decreases with micelle size due to a faster decrease of the cage effect in zero magnetic field.

Our theoretical considerations are based on a set of specific assumptions which include the diffusional motion of the radicals in the micelle and which allow the possibility for the radicals to escape from the micellar boundary with a definite probability once a radical of the pair has reached the micellar boundary. Therefore, we are forced to seek the answers to the questions that we posed in the beginning of the discussion section within the limitations of these assumptions. The first question, concerning the mechanism of the limitation that HFI places on the rate of reaction of nonlabeled pairs in small micelles, arises from the effects of both the frequency of forced reencounters and the ESE between uncoupled electrons of the RP. Both of these factors become more dominant in determining reactivity as the micelle size decreases and as the HFI decreases (an effect that is more important in nonlabeled pairs).

With regard to the question of the role of paramagnetic relaxation in the ISC of the RP, we recognize that the major limitations of our model are its inability to consider HFI with more than a few magnetic nuclei and the possible inappropriateness of the Redfield approach to a very reactive RP in zero magnetic field. However, despite this limitation, the model provides an answer to the issue of magnetic relaxation in a micellized pair: for unlabeled RP (moderate HFI), one may avoid an explicit consideration of paramagnetic relaxation by supposing that the spin levels of the RP are equilibrated at time $t = 0$. For the labeled RP (strong HFI), this suggestion fails to explain the micelle size dependence of the geminate reaction probability. To fit the experimental dependence of P^* on L, we were compelled to explicitly consider the paramagnetic relaxation (DDI and anisotropic HFI) under the assumption of RP in a pure triplet state at $t = 0$, and we found that it is the paramagnetic relaxation due to HFI_{aniso} which is also critical in defining the dependence of the reaction probability of the RP* on micelle size in a strong magnetic field.

In view of our considerations, it is worthwhile to note that any attempt to express the rate constant of reaction in terms of the rate constants of ISC and diffusion (encounters) cannot be used, especially for RP with moderate HFI in small micelles, since such a combination of rate constants has no phenomenological meaning. Actually, the ratio of A/Z is the most important parameter which defines the reaction ability of the RP (Figure 4).

In conclusion, some of the peculiarities of radical reactions in microrestricted micellar environments may be understood through a consideration of simple ideas about intersystem crossing and molecular motion in micelles.

Acknowledgment. The authors thank the National Science Foundation and the Air Force Office of Scientific Research for their generous support of this research. V.F.T. thanks the ICP Co. for financial support.